1 PREDICTING THE DIVERSION LENGTH OF CAPILLARY BARRIERS USING STEADY
2 STATE AND TRANSIENT STATE NUMERICAL MODELING: CASE STUDY OF THE
3 SAINT-TITE-DES-CAPS LANDFILL FINAL COVER

4 Benoit Lacroix Vachon[1], Amir M. Abdolahzadeh[2], and Alexandre R. Cabral[3*]

5   Lacroix Vachon, B., Abdolahzadeh, A.M. and Cabral, A.R. (2015). Predicting the diversion length of capillary barriers using steady state and transient state numerical modeling: Case study of the Saint-Tite-des-Caps landfill final cover. Canadian

6 **Abstract:**   Geotech. J. 52: 2141–2148 (2015) dx.doi.org/10.1139/cgj-2014-0353

7 Covers with capillary barrier effect (CCBE) have already been proposed to meet regulatory

8 requirements for landfill final covers. Modeling of CCBE may be a relatively complex and time

9 consuming task. Simpler, albeit conservative, design tools – such as steady state numerical

10 analyses – can be, in certain cases, justifiable and have a positive impact in the practice. In this

11 study, we performed numerical simulations of the experimental CCBE constructed on the Saint-

12 Tite-des-Caps landfill (Quebec). The CCBE consists of a capillary barrier, composed of sand and

13 gravel, on top of which a layer of deinking by-products (DBP) was installed as a protective layer

14 (also to control seepage). The addition of a protective layer over the infiltration control layer

15 (such as a capillary barrier) is required nearly everywhere. In many European countries, such as

16 Germany and the Netherlands, a thick "recultivation" layer is required. The results of numerical

17 simulations were compared to the *in situ* behaviour of the Saint-Tite CCBE as well as to

18 analytical solutions. The effectiveness of the capillary barrier was assessed by quantifying the

19 diversion length (DL), which reflects the lateral drainage capacity of the CCBE, i.e. the capacity

20 to drain water laterally. The latter, if collected, prevents seepage into the waste mass. This study

[1] P.Eng, M.Sc.A. Groupe Qualitas inc., member of the SNC-LAVALIN group, Montreal, QC, Canada. Formerly with the Department of Civil Engineering, Université de Sherbrooke.
[2] P.Eng., Ph.D. AECOM, Montreal, QC, Canada. Formerly with the Department of Civil Engineering., Université de Sherbrooke.
[3] Department of Civil Engineering, Faculty of Engineering, Université de Sherbrooke, 2500, boul. de l'Université, Sherbrooke, QC J1K 2R1, Canada.
* Corresponding author: A.R. Cabral (Alexandre.Cabral@Usherbrooke.ca).

21 shows that, when the seepage rate reaching the top layer of the capillary barrier is controlled, it is

22 possible to predict the worst case scenario in terms of seepage (and therefore predict the shortest

23 DL) using steady state numerical simulations. These simpler-to-perform numerical simulations

24 could be adopted, at least in a pre-feasibility study for cases with a similar profile as the one at

25 the Saint-Tite-des-Caps experimental CCBE.

26

28

29

30 **Résumé :**

31 Des recouvrements avec effet de barrière capillaire (CCBE) ont déjà été proposés pour répondre

32 aux exigences législatives des recouvrements finaux des sites d'enfouissement. La modélisation

33 d'une CCBE est une tâche relativement complexe et qui peut demander du temps. La possibilité

34 d'effectuer des modélisations numériques plus simples, comme les analyses en régime

35 permanent, tout en offrant une solution conservatrice et éprouvée, pourrait avoir un impact

36 positif dans la pratique. Dans la présente étude, des simulations numériques de la CCBE

37 expérimentale installée au site d'enfouissement de Saint-Tite-des-Caps (Québec) ont été

38 réalisées. La CCBE est constituée d'une barrière capillaire, composée de sable et de gravier, au-

39 dessus de laquelle une couche de sous-produits de désencrage (DBP) a été installée. Cette

40 dernière agissait comme couche de protection et de contrôle des infiltrations. L'ajout d'une

41 couche de protection au-dessus de la barrière capillaire est généralement exigé dans les

42 règlements concernant l'enfouissement de matières résiduelles. Dans certains pays européens,

43 dont l'Allemagne et Les Pays-Bas, on exige une couche épaisse dénommée « recultivation

44   layer ». Les résultats des simulations numériques sont comparés au comportement *in situ* de la

45   CCBE ainsi qu'à certaines solutions analytiques. L'efficacité de la barrière capillaire a été

46   évaluée en quantifiant la longueur de transfert (DL), qui reflète la capacité de drainage latérale de

47   la CCBE. L'eau drainée latéralement doit être captée, évitant ainsi sa percolation vers la masse

48   de déchets. La présente étude démontre que, lorsqu'on contrôle le débit de percolation atteignant

49   la couche supérieure de la barrière capillaire, il est possible de prédire le pire scénario

50   d'infiltration (et donc de prédire la DL la plus courte) par le biais de simulations numériques en

51   régime permanent. Ces simulations numériques plus simples à réaliser pourraient être adoptées,

52   du moins dans le cadre d'une étude de préfaisabilité pour des cas ayant un profil semblable à

53   celui du recouvrement final de la plateforme expérimentale de Saint-Tite-des-Caps.

54

55   Mots-clés : Lieux d'enfouissement sanitaire, sous-produit de désencrage, barrière capillaire,

56   recouvrement final, recouvrement alternatif.

57

1   Introduction

Covers with capillary barrier effect (CCBE) have been proposed as an alternative final cover system for mine residues and waste disposal facilities (Stormont, 1996; Barth and Wohnlich, 1999; Morris and Stormont, 1999; von Der Hude et al., 1999; Khire et al., 2000; Bussière et al., 2003; Kämpf et al., 2003; Wawra and Holfelder, 2003; Aubertin et al., 2006). Regulatory requirements in countries such as Germany and the Netherlands include the addition of a thick layer ("recultivation layer") overlying the capillary barrier (e.g. Giurgea et al., 2003; Hupe et al., 2003) in final covers for solid waste landfills. Relatively fine-textured soils can be employed and therefore become a seepage control layer.

In inclined CCBE, the moisture retaining layer (MRL) diverts (or drains) the rainfall that seeps through the top-most layers of the cover system downslope. The maximum lateral flow the MRL can divert, the diversion capacity (Q_{max}), is attained at a critical zone along the interface called the breakthrough zone. Beyond this zone, capillary forces no longer retain the accumulated water within the MRL; in other words, moisture starts to infiltrate into the capillary break layer (CBL). This transfer of water becomes more accentuated at the diversion length, DL (Ross, 1990), where the downward flow into the CBL (and ultimately into the waste mass) reaches a value equal to the seepage flow rate.

The fundamental design parameters for a CCBE system and the determination of its associated DL are the hydraulic conductivity functions – often derived from the water retention curves (WRC) - of the various layer materials, slope of the cover system, length of the slope, climatic conditions and allowable seepage flow rate. Several authors have discussed how the water

81 storage and lateral diversion capacity of a capillary barrier is affected by factors such as the

82 material properties and thickness, cover configuration, slope of the interface, and climatic

83 conditions (Morris and Stormont, 1998; Zhan et al., 2001; Tami et al., 2004; Parent and Cabral,

84 2006; Yanful et al., 2006; Aubertin et al., 2009).

85

86 Depending on climatic conditions, the amount of precipitation that infiltrates through the surface

87 may exceed the water storage capacity of the MRL and the diversion capacity of the CCBE,

88 thereby limiting lateral drainage within the MRL and hence reducing the diversion length.

89 Abdolahzadeh et al. (2011a; 2011b) suggested adding a seepage control layer on top of the MRL

90 in order to limit the seepage flow rate to a maximum equal to the saturated hydraulic

91 conductivity of the seepage control layer. It needs, nonetheless, to be acknowledged that the

92 maximum flow rate may be dictated by the presence of cracks within the seepage control layer.

93

94 In this study, transient state numerical simulations were performed based on the experimental

95 CCBE constructed on the Saint-Tite-des-Caps landfill (Lacroix Vachon et al., 2007;

96 Abdolahzadeh et al., 2008; Abdolahzadeh et al., 2011a; Abdolahzadeh et al., 2011b). The results

97 of the numerical simulations under transient state were compared to the response of the

98 experimental CCBE for a typical year (Abdolahzadeh et al., 2011a; Abdolahzadeh et al., 2011b),

99 to the results obtained by steady state numerical simulations, to the results obtained using a well-

100 known analytical solution (Ross, 1990), and to the results obtained using an adaptation of the

101 latter (Parent and Cabral, 2006).

102

103 Transient-state numerical simulations better define the behaviour of a CCBE and therefore

104 constitute a more precise design tool. This is partly attributed to the fact that the precipitation

105 rate changes continuously, thus the seepage flow rate reaching the top of the CCBE and the

106 suctions at the interface between the MRL and CBL change accordingly. As a consequence, it is

107 expected that the diversion length varies continuously and the design process needs to consider

108 these naturally-occurring variations. Despite this fact, the results reported in this paper show that

109 when the seepage flow rate level can be controlled, a steady state analysis can predict the worst-

110 case scenario in terms of diversion length, and can therefore be considered at least for the pre-

111 design (feasibility) phase of a project.

112

113 ## 2   Materials and Methods

114 ### 2.1   Composition of the materials

115 The longitudinal profile of the 10-m wide and 30-m long experimental cover installed at the

116 Saint-Tite-des-Caps landfill site was presented by Abdolahzadeh et al. (2011a), who describe the

117 instrumentation installed in it. The upper layer, constructed with random fill, protects the lower

118 layers and is required by Quebec landfill regulations. The immediately underlying layer consists

119 of deinking by-products DBP (0.6 m) and forms a hydraulic barrier (or seepage control barrier).

120 The lower part of the experimental final cover includes a capillary barrier made up of a layer of

121 sand (0.4 m) superposed over a layer of gravel (0.2 m).

122

123   The water retention curve of DBP (whose Gs = 2.0) was obtained using a pressure plate modified

124   by Parent (2006) to test highly compressible materials (Cabral et al., 2004; Parent et al., 2004;

125   Parent et al., 2007). The experimental results and a fitting curve using the Fredlund and Xing

126   (1994) model are presented in Figure 1. The corresponding Fredlund and Xing (1994) parameters

127   fitting curve and the saturated volumetric water content (θ_s) value for DBP are presented in

128   Table 1. The porosities (n) of all the materials are equal to their saturated volumetric water

129   contents (θ_s in Table 1). The WRCs of the sand (Gs=2.65) and gravel (Gs=2.65) were obtained

130   by means of drainage columns (Lacroix Vachon, 2008; Abdolahzadeh et al., 2011a).

131

132   The van Genuchten model (1980) was selected as the regression model for the sand and gravel

133   (Figure 1a) and their corresponding van Genuchten parameters are presented in Table 1. Data for

134   the WRC of the waste was taken from the GeoStudio (Geo-Slope Int. Ltd., 2004) database. The

135   main hydraulic properties of the waste, including the van Genuchten (1980) corresponding

136   parameters, are also summarized in Table 1, which also presents the air entry values (ψ_{AEV}) and

137   water entry values (ψ_{WEV}) of most of the different materials employed. These values were

138   determined using the Brooks and Corey (1964) graphical method.

139

140   The saturated hydraulic conductivity (k_{sat}) of DBP is equal to 1.0 x 10^{-8} m/s, as obtained by

141   Bédard (2005), Burnotte et al. (2000) and Planchet (2001). The saturated hydraulic conductivity

142   of the sand, 1.5 x 10^{-4} m/s, was estimated using the Hazen (1911) formula, with a cross-check

143   using the neural network in the RETC code (van Genuchten et al., 1991). For the gravel, the k_{sat}

144   (1.5 x 10^{-3} m/s) was also estimated with the Hazen (1911) formula, with a cross-check using the

145   Chapuis (2004) method. The k_{sat} values are presented in Table 1. The k-fct of the sand, gravel

146   and waste, shown in Figure 1b, were obtained using the van Genuchten (1980) model, based on

147   the Mualem (1976) formulation.

148

149   In the present study, the effect of hysteresis of the WRC was not considered; only the drying

150   curve was used. Zhang et al. (2009) showed that pore water pressure distributions in modeled

151   capillary barriers, as well as the DL location, are influenced by whether or not hysteresis is

152   considered. While it can be important for fine sands, an investigation performed by Maqsoud et

153   al. (2004) showed that for coarse-grained materials, this effect is much less important.

154

155

156   Table 1: Hydraulic properties of the materials used in numerical simulations of the Saint-Tite-
157   des-Caps experimental CCBE.

158

159   Figure 1: a) Water retention curve (WRC); and b) *k-fct* of the materials used in numerical
160   simulations.

161

162

163   **2.2   Analytical solutions and numerical modeling**

164   **2.2.1   Analytical solutions**

165   Various equations can be used to evaluate the DL, such as those proposed by Ross (1990),

166   Steenhuis et al. (1991), Morel-Seytoux (1994) and Walter et al. (2000). Ross (1990) developed

167   analytical relationships for the DL and Q_{max} of a capillary barrier and applied equations based on

168   constant infiltration into the fine layer and semi-infinite layers of soil. According to the Ross

169 (1990) model, water that accumulates at the interface between the MRL and the CBL only starts

170 to flow down when suction reaches a critical value. Steenhuis et al. (1991) suggested that the

171 critical suction value can be considered the water entry value (WEV) of the CBL, i.e. ψ_{WEV}^{CBL}. This

172 parameter corresponds to the suction value at which the downward flow into the CBL (q_d)

173 becomes equal to the seepage flow rate (q). Various studies have shown that the critical suction

174 value definition suggested by Steenhuis et al. (1991) is more widely retained (Walter et al., 2000;

175 Bussière et al., 2002; Nakafusa et al., 2012).

176

177 Based on the Ross (1990) model, the critical suction value is the suction at which the *k-fcts* of the

178 MRL and CBL intersect. According to this analytical solution, the fine-grained material drains

179 all the water down to the point where the critical suction value is attained. Abdolahzadeh et al.

180 (2011b; 2011a), Parent and Cabral (2006), among others, presented evidence – based on field

181 data and numerical simulations - that the downward flow into the CBL occurs gradually, often in

182 a sigmoidal manner with distance. Considering this, Parent and Cabral (2006) developed a

183 methodology based on the Ross (1990) model and proposed an empirical equation to quantify

184 seepage flow into the CBL, taking into consideration a progressive downward flow into the

185 coarse-grained material.

186

187 **2.2.2   Numerical simulations**

188

189 Numerical modeling of the Saint-Tite-des-Caps CCBE was performed in two distinct steps. In

190 the first, the hydrological behaviour of the first two layers was investigated using Visual HELP

191 (v. 2.2.03; Schlumberger Water Services), which considers the climate-dependent processes of

9

192   precipitation, evapotranspiration and runoff. Visual HELP simulated the annual percolation rates

193   reaching the top of the sand/gravel capillary barrier. In the second step, the unsaturated flow

194   through the CCBE was simulated using SEEP/W (v. 2007; Geo-Slope Int. Ltd.). The simulated

195   annual percolation rates obtained by Visual HELP were introduced in SEEP/W as an upper

196   hydraulic boundary condition, for transient numerical simulations. For the steady state numerical

197   simulation, the percolation rate value was fixed at 1×10^{-8} m/s, i.e. the k_{sat} of DBP.

198

199   **2.2.3   Seepage flow rate reaching the capillary barrier: role of the seepage control layer**

200

201   Abdolahzadeh et al. (2011a) analyzed field data from Saint-Tite-des-Caps experimental CCBE

202   and found that the DBP layer diverts water laterally over a very short distance (less than 2.6 m),

203   remaining saturated most of the time and along almost the entire length of the CCBE.

204   Consequently, the DBP layer controls the amount of seepage reaching the sand/gravel capillary

205   barrier. In order to evaluate this amount of seepage, the software Visual Help was used. Climatic

206   data was obtained using a weather station (Vantage Pro; Davis Instruments) and was completed

207   using the Visual HELP database (data from Quebec City). The main input data for the Visual

208   HELP simulations are summarized in Table 2. A 5% slope was assigned to the model. The field

209   capacity and wilting point moisture content input parameters, which are used to define moisture

210   storage and unsaturated hydraulic conductivity, were obtained using the WRC. In all unsaturated

211   layers, the initial moisture content was assumed equal to the wilting point value (Webb, 1997).

212   Based on the results obtained from the Visual HELP simulations, the median year was adopted

213   as typical year.

214

215

216   Table 2: Summary of HELP simulations input.

217

2.2.4   Geometry and boundary conditions of the capillary barrier model

219

220   Only the capillary barrier system consisting of sand and gravel that superimposes a layer of

221   typical municipal solid waste was modelled in the present study. Given the fact that the DBP

222   remained saturated at its base, a seepage boundary condition at the top of the sand layer was

223   considered. The geometry and dimensions for the slightly inclined capillary barrier modelled

224   herein are illustrated in Figure 2. The arbitrary thickness of the waste layer (0.5 m) was of little

225   importance in the final results, given the coarse nature of this layer; i.e. the waste was not able to

226   transmit any significant suction to the gravel layer, given the simulated seepage flow rate. The

227   mesh density was adapted to improve the solution accuracy in critical zones, particularly at the

228   sand-gravel interface (Chapuis, 2012). As it can be observed in Figure 2, various mesh densities

229   were adopted. The vertical thickness of the elements near the sand-gravel interface and waste

230   layer were 0.09 m and 0.25 m respectively. The horizontal length of the elements was similar

231   throughout the model. A zero seepage horizontal flow was adopted at the upstream vertical

232   boundary, which corresponds to the reality of the field experiment. A rectangular form was

233   considered because it helped to achieve numerical stability. To avoid boundary effects on the

234   right side of the model, the toe of the capillary barrier model was extended up to 200.0 m

235   horizontally (Figure 2).

236

237 Three types of boundary conditions were used to simulate the Saint-Tite-des-Caps CCBE and are

238 illustrated in Figure 2. At the downstream end of the model, two drains were located in the sand

239 and gravel layers. These drainage outlets were simulated by applying a unit hydraulic gradient

240 boundary. The physical meaning of this boundary condition was that the seepage flow rate that

241 passed through the drainage outlet boundary at a given suction value was equal to the coefficient

242 of permeability of the soil corresponding to that suction value (Tami et al., 2004). The water

243 table was placed at the base of the waste layer, at a depth of 110 cm from the ground surface

244 layer. A zero pressure boundary condition was imposed, representing the worst case (in fact,

245 virtually impossible) scenario. It is assumed that maximum suction the wastes can transmit to the

246 CBL is low enough so that the suction at the CBL-MRL interface is not affected by it.

247 Accordingly, the shape of the WRC of the wastes does not affect the behaviour of the capillary

248 barrier.

249

250 For the transient analysis, the initial pressure head at each node was obtained from the steady

251 state simulation. The behaviour of the capillary barrier model was analyzed using wet initial

252 conditions. This was considered as the worst condition, insofar as the capillary barrier model had

253 a low storage capacity.

254

255

256 Figure 2: Basic model, geometry, dimensions, and boundary conditions of the Saint-Tite-des-
257 Caps CCBE.

258

3   Results

3.1   Potential seepage flow rates

261   Lysimeters were installed in the sand layer to monitor the maximum amounts of water entering

262   the sand/gravel capillary barrier for several years. A verification of their functionality was

263   performed by Abdolahzadeh et al. (2011b), who concluded that, except for short periods of time,

264   the lysimeters performed properly, i.e. suctions were equal to zero at the base and, at the top,

265   their values were the same inside and immediately on the outside; in other words, there were no

266   differences in total heads that could cause deviation or concentration of flow. As can be seen in

267   Figure 3, field observations clearly indicated that the maximum seepage flow rate throughout

268   2006 (adopted year) did not exceed 1.0×10^{-8} m/s, i.e. the k_{sat} of DBP.

269

270

271   Figure 3: Evolution of seepage flow rates reaching the top of the sand/gravel capillary barrier by
272   lysimeters installed in the sand layer at the Saint-Tite-des-Caps experimental CCBE, for year
273   2006 (adapted from Abdolahzadeh et al., 2008).
274

275

276   The results of the Visual HELP simulations are presented in Figure 4 for a typical simulated

277   year. Seepage rate values equal to 1.9×10^{-8} m/s were sometimes obtained by the modeling

278   process. Since they were not corroborated by field observations (Figure 3), seepage values

279   greater than 1.0×10^{-8} m/s were set to 1.0×10^{-8} m/s. The seepage flow rates adopted as the

280   upper boundary condition for the unsaturated flow simulations under transient state are indicated

281   in Figure 4.

282

283   Figure 4: Visual HELP modeling results of the seepage flow rates through the DBP
284   layer during a typical year.

285

286   **3.2   Unsaturated flow simulations to determine DL**

287   One of the goals of the numerical simulations was to estimate the approximate location of the

288   diversion length along the sand/gravel capillary barrier. For practical purposes, instead of a

289   region, the DL is associated herein with a precise distance from the top of the slope. The DL is

290   located where the suction along the sand/gravel interface reaches the critical suction value ψ_{WEV}

291   of the CBL (Steenhuis et al., 1991). From this location downslope, the suction at the interface

292   tended to stabilize. In the present study, the diversion length was evaluated using 5 different

293   approaches: 1) field data gathered from the Saint-Tite-des-Caps experimental CCBE; 2) a steady

294   state numerical simulation; 3) a transient-state numerical simulation; 4) the Ross (1990)

295   analytical model; and 5) the Parent and Cabral (2006) analytical model.

296

297   During the spring and summer of 2006, the DL at the Saint-Tite-des-Caps experimental CCBE

298   was evaluated based on lysimeter, tensiometer and water content data. According to

299   Abdolahzadeh et al. (2011b), the DL was located between 23.0 and 29.0 m (Figure 5). As

300   observed by Abdolahzadeh et al. (2011a), suction values did stabilize downslope from the

301   approximate DL region.

302

303 The seepage flow rates obtained from the transient and steady state analyses are also presented in

304 Figure 5. It can be observed that when the flow rate value falls below 1.0×10^{-8} m/s, the DL

305 given by the transient analysis increased accordingly. The lowest DL value obtained from the

306 transient analysis was equal to the value obtained from the steady state analysis (DL = 19.0 m).

307

308 For the sake of comparison, the DL obtained using the Ross (1990) and Parent and Cabral (2006)

309 models are also included in Figure 5. The Parent and Cabral (2006) model, with a DL=20.0 m,

310 compared very well with the steady state DL, while the Ross (1990) model gave a very

311 conservative DL value equal to 16.0 m. The very conservative nature of the DL by the Ross

312 model results in part from the fact that this model is based on an "all-or-nothing" type of

313 approach when it comes to determining the transfer capacity of the MRL and the diversion

314 length.

315

316 In concluding, the lowest value of DL from the transient state analysis was equal to the DL

317 obtained by modeling the CCBE under steady state and this value was quite close to what was

318 actually observed in the field for the typical year analyzed. It is therefore tempting to conclude

319 that steady state analyses could be a practical and effective choice for the design of CCBEs.

320 Indeed, this can be the case under the following circumstances: when a CCBE is designed to

321 minimize water infiltration and when a low permeability layer is installed above the MRL as a

322 means to control the maximum seepage reaching it. Therefore, the maximum seepage flow

323 reaching the MRL is equal to the k_{sat} of the seepage control layer. Zhang et al. (2004) observed

324 that in order to maintain negative pore-water pressure values in a slope, it is important to reduce

325 the infiltration flux through the use of a suitable type of cover system at the ground surface. Lim

326 et al. (1996) carried out a field instrumentation program to monitor negative pore-water pressure

327 values in residual soil slopes in Singapore that were protected by different types of surface

328 covers. The changes in matric suction due to changes in ground surface moisture flux were found

329 to be least significant under a canvas-covered slope and most significant in a bare slope. Several

330 relatively impermeable surface covers can be adopted.

331

332

333 Figure 5: Evolution of the diversion length, as a function of the seepage flow rate (modified
334 Visual HELP results, indicated as **"adopted"**; see Figure 4) and evolution of DL
335 obtained by transient and, steady state analysis, as well as by using the Parent and
336 Cabral (2006) and Ross (1990) models.

337

338 The level of confidence associated with the DL values obtained is intimately related to the level

339 of confidence associated with the properties of the materials, the boundary conditions and initial

340 conditions imposed on the model. It is therefore noteworthy that the DL obtained perfectly

341 corroborates what was obtained by Abdolazadeh et al. (2011a) using lysimeter and tensiometer

342 data. The accurateness of the material's properties was assessed by Abdolahzadeh et al. (2011b).

343

344 **4 Conclusion**

345 The design of CCBE is complex due to its transient behaviour, and several studies conclude that

346 numerical simulations under transient states may better define the response of CCBE than those

347 obtained from steady-state numerical or analytical solutions. Nevertheless, steady state solutions

348 (numerical or analytical), associated with simplified assumptions and combined with particular

349 boundary conditions, may allow engineers to make reasonable predictions using simple tools,

350 thereby circumventing the difficulties and time involved to model a system under transient state.

351

352 The most important result of the research reported in this paper is that the DL obtained under

353 steady state coincided with the worst-case scenario (in terms of diversion length) predicted by

354 transient analysis, for the particular conditions of the Saint-Tite-des-Caps experimental CCBE.

355 And it is relevant to note that the predicted DL was confirmed by field data. The present study

356 concluded that steady state numerical analysis or an analytical solution such as Parent and Cabral

357 (2006) predicts a conservative diversion length and, therefore, it is possible to use them during

358 the preliminary design phase of a cover system that controls seepage into the waste mass.

359

360

361 ## Acknowledgements

367

368

369 ## References

370   Abdolahzadeh, A.M., Lacroix Vachon, B. and Cabral, A.R. (2008). Hydraulic barrier and its

371   impact on the performance of cover with double capillary barrier effect *In 61st Canadian*

372   *Geotechnical Conference*. Edmonton. 21-24 Sept., CD-Rom.

373   Abdolahzadeh, A.M., Vachon, B.L. and Cabral, A.R. (2011a). Evaluation of the effectiveness of

374   a cover with capillary barrier effect to control percolation into a waste disposal facility.

375   *Canadian Geotechnical Journal*, **48**(7), 996-1009.

376   Abdolahzadeh, A.M., Vachon, B.L. and Cabral, A.R. (2011b). Assessment of the design of an

377   experimental cover with capillary barrier effect using 4 years of field data. *Geotechnical*

378   *and Geological Engineering*, **29**(5), 783-802.

379   Aubertin, M., Cifuentes, E., Apithy, S.A., Bussière, B., Molson, J. and Chapuis, R.P. (2009).

380   Analyses of water diversion along inclined covers with capillary barrier effects.

381   *Canadian Geotechnical Journal*, **46**(10), 1146-1164.

382   Aubertin, M., Cifuentes, E., Martin, V., Apithy, S., Bussiere, B., Molson, J., Chapuis, R.P. and

383   Maqsoud, A. (2006). An investigation of factors that influence the water diversion

384   capacity of inclined covers with capillary barrier effects. Carefree, AZ, United States,

385   Geotechnical Special Publication 147, American Society of Civil Engineers, Reston, VA

386   20191-4400, United States, 613-624.

387   Barth, C. and Wohnlich, S. (1999). Proof of effectiveness of a capillary barrier as surface sealing

388   of sanitary landfill. *In 7th International Waste Management and Landfill Symposium*.

389   *Edited by* R. Cossu, R. Stegman, and T.H. Christensen. Sant Margarita di Pula, Italy,

390   389-392.

391 Bédard, D. (2005). Effet du fluage à long terme des sous-produits de désencrage dû à la perte de

392 masse et son effet sur la compression et la conductivité hydraulique. M.Sc.A Thesis,

393 Université de Sherbrooke, Sherbrooke, 166 p.

394 Brooks, R.H. and Corey, A.T. (1964). Hydraulic properties of porous media. *Hydrology paper*

395 *no. 3, Colorado State University, Fort Collins, Colorado*.

396 Burnotte, F., Lefebvre, G., Cabral, A., Audet, C. and Veilleux, A. (2000). Use of deinking

397 residues for the final cover of a MSW landfill. *In 53rd Canadian Geotechnical*

398 *Conference*. Montreal. October 15-18, 2000, Vol. 1, 585-591.

399 Bussière, B., Aubertin, M. and Chapuis, R.P. (2002). A laboratory set up to evaluate the

400 hydraulic behavior of inclined capillary barriers. *In International Conference on Physical*

401 *Modelling in Geotechnics. Edited by* R. Phillips, P.J. Guo, and R. Popescu. St. John's,

402 Newfoundland. July 2002, 391-396.

403 Bussière, B., Apithy, S., Aubertin, M. and Chapuis, R.P. (2003). Diversion capacity of sloping

404 covers with capillary barrier effect. *In* 56th Annual Canadian Geotechnical Conf., 4th Joint

405 IAH-CNC and CGS Groundwater Specialty Conf. & 2003 NAGS Conference, Winnipeg,

406 Canada, p. 8,

407 Cabral, A.R., Planchet, L., Marinho, F.A. and Lefebvre, G. (2004). Determination of the soil

408 water characteristic curve of highly compressible materials: case study of pulp and paper

409 by-product. *Geot. Testing Journal*, **27**(2), 154-162.

410 Chapuis, R.P. (2004). Predicting the saturated hydraulic conductivity of sand and gravel using

411 effective diameter and void ratio. *Canadian Geotechnical Journal*, **41**(5), 787-795.

412 Chapuis, R.P. (2012). Influence of element size in numerical studies of seepage: unsaturated

413 zones, transient conditions. *Geotechnical News*, BiTech, Dec., 34-37 p.

414 Fredlund, D.G. and Xing, A.Q. (1994). Equations for the soil-water characteristic curve.

415   *Canadian Geotechnical Journal*, **31**(4), 521-532.

416 Geo-Slope (2004). SEEP/W User's Manual,

417 Giurgea, V.I., Hötzl, H. and Breh, W. (2003). Studies on the long-term performance of an

418   alternative surface-sealing system with underlying capillary barrier *In Sardinia 2003 - 9th*

419   *International Landfill Symposium*. *Edited by* R. Cossu and R. Stegmann. St-Margarita di

420   Pula, Italy. Oct. 2003, CISA, Paper 307 - CD-Rom.

421 Hazen, A. (1911). Discussion of "Dams on Sand Foundations" from A.C. Koening. *ASCE*, **73**.

422 Hupe, K., Heyer, K.-U., Becker, J.F., Traore, O., Noetzel, S. and Stegmann, R. (2003).

423   Investigations of alternative landfill surface sealing systems in test fields *In Sardinia*

424   *2003 - 9th International Landfill Symposium*. *Edited by* R. Cossu and R. Stegmann. St-

425   Margarita di Pula, Italy. Oct. 2003, CISA, Paper 582 - CD-Rom.

426 Kämpf, M., Holfelder, T. and Montenegro, H. (2003). Identification and parameterization of

427   flow processes in artificial capillary barriers. *Water Resources Research*, **39**(10), 21-29.

428 Khire, M.V., Benson, C.H. and Bosscher, P.J. (2000). Capillary barriers: Design variables and

429   water balance. *Journal of Geotechnical and Geoenvironmental Engineering*, **126**(8), 695-

430   708.

431 Lacroix Vachon, B. (2008). Les écoulements dans les milieux non saturés et leurs applications

432   aux couvertures avec effet de barrière capillaire installées dans un site d'enfouissement

433   sanitaire Dissertation Thesis, Université de Sherbrooke, Sherbrooke, 138 p.

434 Lacroix Vachon, B., El-Ghabi, B. and Cabral, A.R. (2007). Évaluation préliminaire de

435   l'efficacité du recouvrement avec double effet de barrière capillaire installé au site de St-

436   Tite-des-Caps, Qc. *In 60th Canadian Geotechnical Conference*. Ottawa. 21-24 Oct., Vol.

437   CD-Rom.

438   Lim, T.T., Rahardjo, H., Chang, M.F. and Fredlund, D.G. (1996). Effect of rainfall on matric

439   suctions in a residual soil slope. *Canadian Geotechnical Journal*, **33**(4), 618-628.

440   Maqsoud, A., Bussière, B. and Aubertin, M. (2004). Hysteresis effects on the water retention

441   curve: a comparison between laboratory results and predictive models. *In 57th Canadian*

442   *Geotechnical Conference and the 5th Joint CGS-IAH Conference*. Quebec City, Canada,

443   CGS, Vol. Session 3A, 8-15.

444   Morel-Seytoux, H.J. (1994). Steady-state effectiveness of a capillary barrier on a sloping

445   interface. *In 14th Hydrology Days*. *Edited by* H.J. Morel-Seytoux. Atherton, CA,

446   Hydrology Days Publications, 335-346.

447   Morris, C.E. and Stormont, J.C. (1998). Evaluation of numerical simulations of capillary barrier

448   field tests. *Geotechnical and Geological Engineering*, **16**, 201-213.

449   Morris, C.E. and Stormont, J.C. (1999). Parametric study of unsaturated drainage layers in a

450   capillary barrier. *Journal of Geotechnical & Geoenvironmental Engineering*, **125**(12),

451   1057-1065.

452   Mualem, Y. (1976). A new model for predicting the hydraulic conductivity of unsaturated porous

453   media. *Water Resources Research*, **12**, 513-522.

454   Nakafusa, S., Kobayashi, K., Morii, T. and Takeshita, Y. (2012). Estimation of water diversion

455   provided by capillary barrier of soils. *In 5th Asia-Pacific Conference on Unsaturated Soils*

456   *2012*. Pattaya, Thailand. Feb. 29 - March 2, 2012, Geotechnical Engineering Research

457   and Development Center, Vol. 2, 643-647.

458   Parent, S.-É. (2006). Aspects hydrauliques et géotechniques de la conception de barrières

459   capillaires incluant des matériaux recyclés hautement compressibles. Dissertation/Thesis

460   Thesis, Université de Sherbrooke, Sherbrooke, 114 p.

461   Parent, S.-É. and Cabral, A.R. (2006). Design of inclined covers with capillary barrier effect.

462   *Geotechnical and Geological Engineering Journal*, **24**, 689-710.

463   Parent, S.-É., Cabral, A.R. and Zornberg, J.G. (2007). Water retention curves and hydraulic

464   conductivity functions of highly compressible materials. *Canadian Geotechnical Journal*,

465   **44**(10), 1200-1214.

466   Parent, S.-É., Cabral, A.R., Dell' Avanzi, E. and Zornberg, J.G. (2004). Determination of the

467   hydraulic conductivity function of a highly compressible material based on tests with

468   saturated samples. *Geot. Testing Journal*, **27**(6), 1-5.

469   Planchet, L. (2001). Utilisation des résidus de désencrage comme barrière capillaire et

470   évapotranspirative (ET) pour les parcs à résidus miniers producteurs de DMA Thesis,

471   Université de Sherbrooke, Sherbrooke, 114 p.

472   Ross, B. (1990). Diversion capacity of capillary barriers. *Water Resources Research*, **26**(10),

473   2625-2629.

474   Steenhuis, T.S., Parlange, J.Y. and Kung, K.J.S. (1991). Comment on 'the diversion capacity of

475   capillary barriers' by Benjamin Ross (paper 91WR01366). *Water Resources Research*,

476   **27**(8), 2155.

477   Stormont, J.C. (1996). The effectiveness of two capillary barriers on a 10% slope. *Geotechnical*

478   *and Geological Engineering Journal*, **14**, 243-267.

479   Tami, D., Rahardjo, H., Leong, E.C. and Fredlund, D.G. (2004). Design and laboratory

480   verification of a physical model of sloping capillary barrier. *Canadian Geotechnical*

481   *Journal*, **41**, 814 - 830.

482   van Genuchten, M.T. (1980). A closed-form equation for predicting the hydraulic conductivity of

483   unsaturated soils. *Soil Science Society of America Journal*, **44**, 892-898.

484   van Genuchten, M.T., Leij, F.J. and Yates, S.R. (1991). The RETC code for quantifying the

485   hydraulic functions of unsaturated soils. In: (eds), Report EPA/600/2-91/065, U.S.

486   Department of Agriculture, Agriculture Research Service p.

487   von Der Hude, N., Melchior, S. and Möckel, S. (1999). Construction of a capillary barrier in the

488   cover of the Breinermoor landfill. *In Seventh International Waste Management and*

489   *Landfill Symposium. Edited by* T.H. Christensen, R. Cossu, and R. Stegmann. Sta

490   Margarita di Pula, Italy, CISA, 393-402.

491   Walter, M.T., Kim, J.S., Steenhuis, T.S., Parlange, J.Y., Heilig, A., Braddock, R.D., Selker, J.S.

492   and Boll, J. (2000). Funneled flow mechanisms in a sloping layered soil: Laboratory

493   investigation. *Water Resources Research*, **36**(4), 841-849.

494   Wawra, B. and Holfelder, T. (2003). Development of a landfill cover with capillary barrier for

495   methane oxidation - the capillary barrier as gas distribution layer. *In 9th Int. Waste Mgmt*

496   *and Landfill Symp.* Italy. October 6-10, 2003, Paper 348.

497   Webb, S.W. (1997). Generalization of Ross Tilted Capillary Barrier Diversion Formula for

498   Different Two-Phase Characteristic Curves. *Water Resources Research*, **33**(8), 1855-

499   1859.

500   Yanful, E.K., Mousavi, M. and De Souza, L.P. (2006). A numerical study of soil cover

501   performance. *Journal of Environmental Management*, **81**, 72–92.

502   Zhan, G., Mayer, A., McMullen, J. and Aubertin, M. (2001). Slope effect study on the capillary

503   cover design for a spent leach pad. *In 8th International Conference Tailings and Mine*

504   *Waste '01*. Colorado State University, Forth Collins, Co., Balkema, 179-187.

505   Zhang, L.L., Fredlund, D.G., Zhang, L.M. and Tang, W.H. (2004). Numerical study of soil

506   conditions under which matric suction can be maintained. *Canadian Geotechnical*

507   *Journal*, **41**, 569–582.

508   Zhang, Q., Werner, A., Aviyanto, R. and Hutson, J. (2009). Influence of soil moisture hysteresis

509   on the functioning of capillary barriers. *Hydrological Processes*, **23**, 1369-1375.

510

511

Tables

Table **1**: Hydraulic properties of the materials used in numerical simulations of the Saint-Tite-des-Caps experimental CCBE.

Parameters	DBP	Sand	Gravel	Waste
WRC's model	FX [1]	vG [2]	vG [2]	vG [2]
α [3] [4]	45.5	0.472	1.953	0.38
n [3]	1.42	6.32	4.20	1.47
m [3]	0.876	0.842	0.762	0.32
Cr (kPa) [5]	2000	n/a	n/a	n/a
θ_s (m³/m³)	0.77	0.33	0.35	0.30
θ_r (m³/m³)	n/a	0.05	0.07	0.01
k_{sat} (m/s) [6]	1×10^{-8}	1.5×10^{-4}	1.5×10^{-3}	1.0×10^{-5}
ψ_{AEV} (kPa) [7]	~ 14	~ 1.4	~ 0.4	~ 2.6
ψ_{WEV} (kPa) [8]	---	~ 3.5	1.7 [9]	~ 200

Note:

[1] FX: Fredlund and Xing (1994);

[2] vG: van Genuchten (1980);

[3] α, n, m are van Genuchten (1980) parameters;

[4] 1/kPa for van Genuchten model, kPa for Fredlund and Xing model;

[5] Cr: in Fredlund and Xing (1994) model, this parameter is a constant derived from the residual suction, i.e. the tendency to the null water content;

[6] k_{sat} is saturated hydraulic conductivity;

[7] ψ_{AEV} is the suction value at air entry value;

[8] ψ_{WEV} is the suction value at water entry value;

[9] Rounded value.

Table **2**: Summary of HELP simulations input.

Layer	Thickness (m)	Properties	HELP layer type	Total porosity (vol/vol)	Field capacity (vol/vol)	Wilting point (vol/vol)	k_{sat} (m/s)	Subsurface inflow (mm/year)
Loamy fine sand	0.6	Top soil (protection layer)	Vertical percolation	0.453	0.19	0.085	7.2×10^{-6}	0
DBP	0.6	Barrier soil (seepage control layer)	Barrier soil liner	0.775	0.71	0.231	1.0×10^{-8}	0

Figures
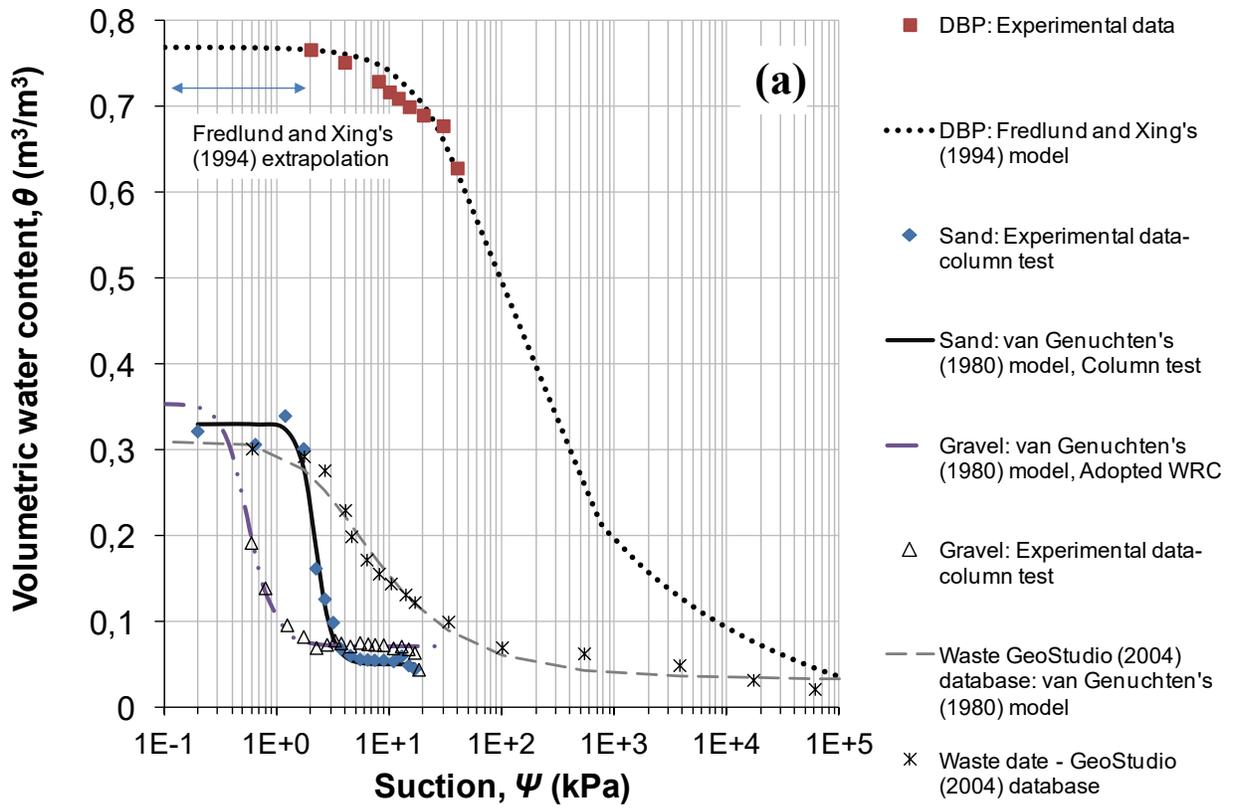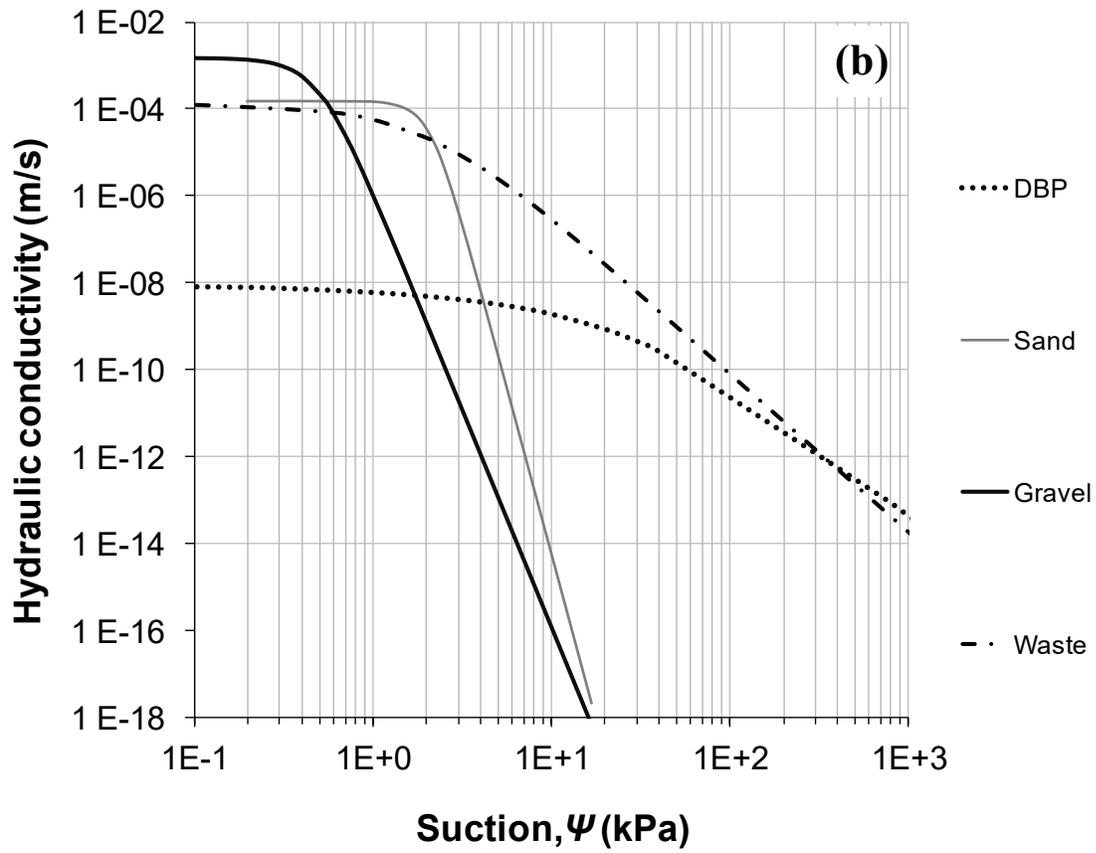
Figure 1: a) Water retention curve (WRC); and b) *k-fct* of the materials used in numerical simulations.
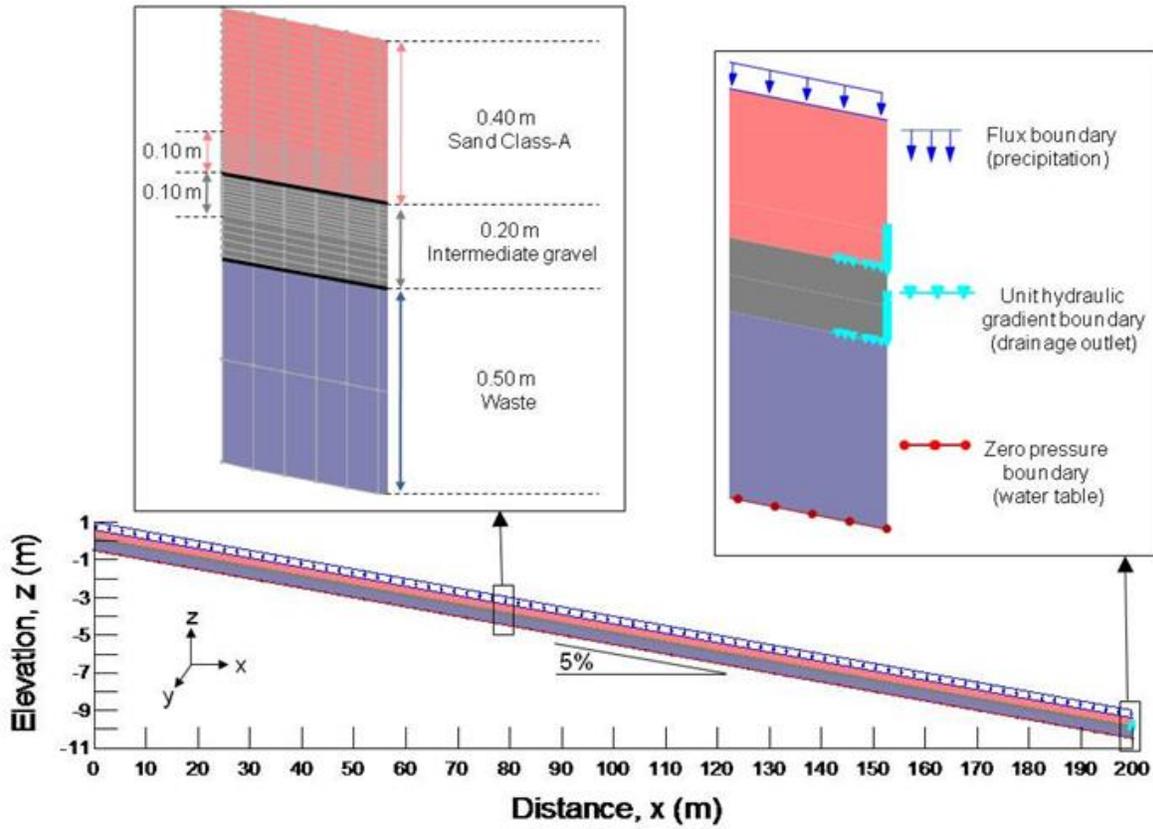
Figure 2: Basic model, geometry, dimensions, and boundary conditions of the Saint-Tite-des-Caps CCBE.
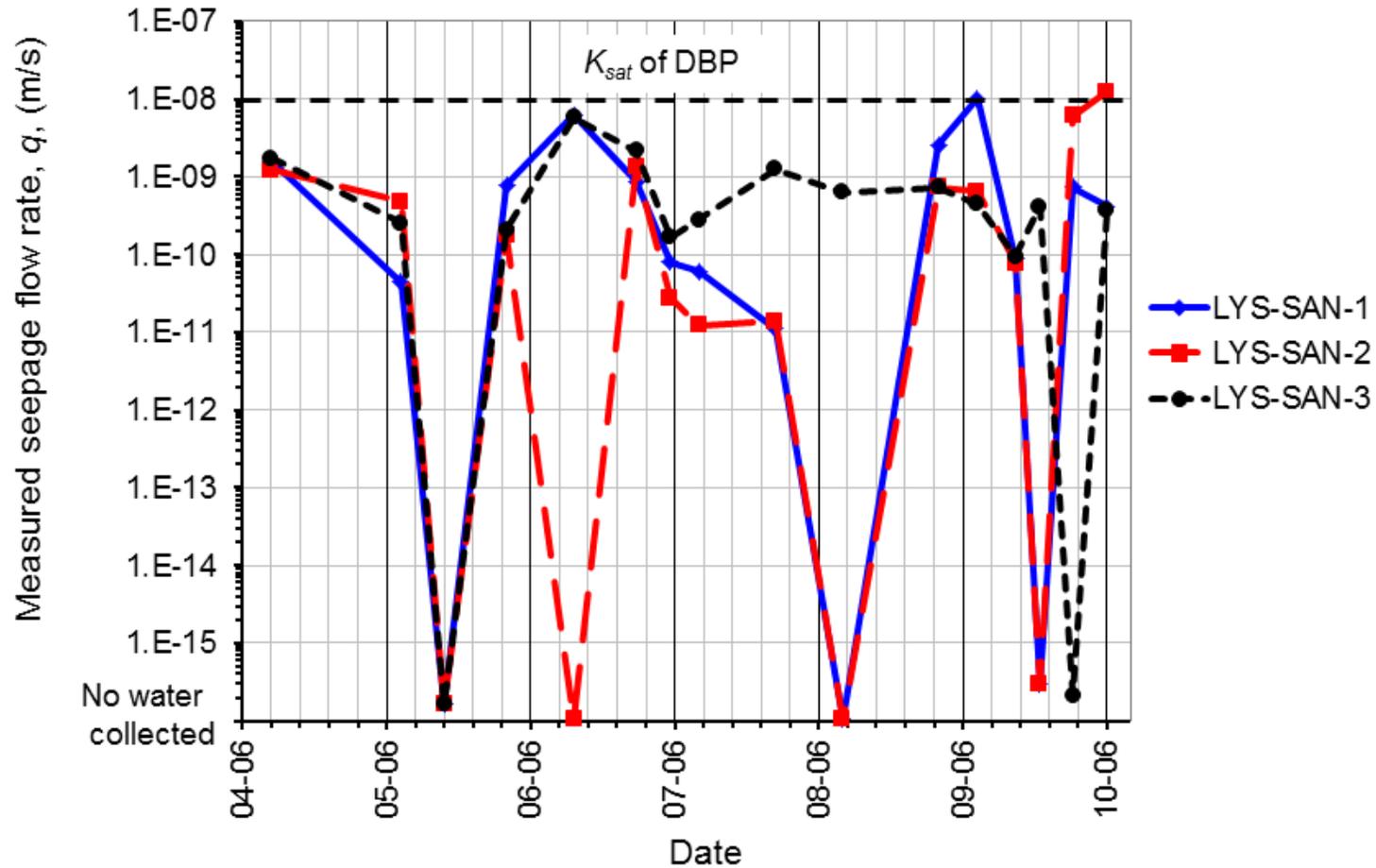
Figure 3: Evolution of seepage flow rates reaching the top of the sand/gravel capillary barrier by lysimeters installed in the sand layer at the Saint-Tite-des-Caps experimental CCBE, for year 2006 (adapted from Abdolahzadeh et al., 2008).
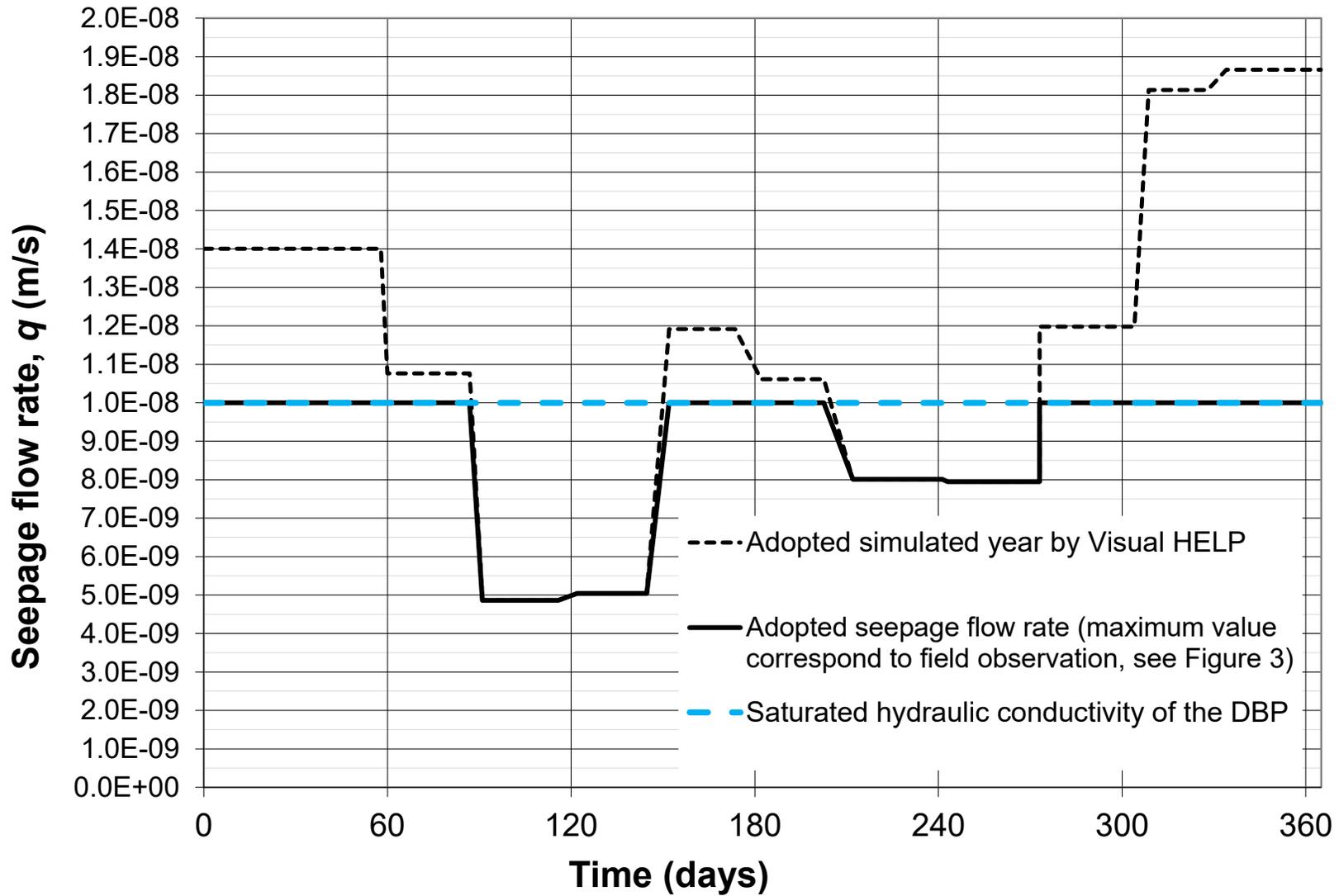
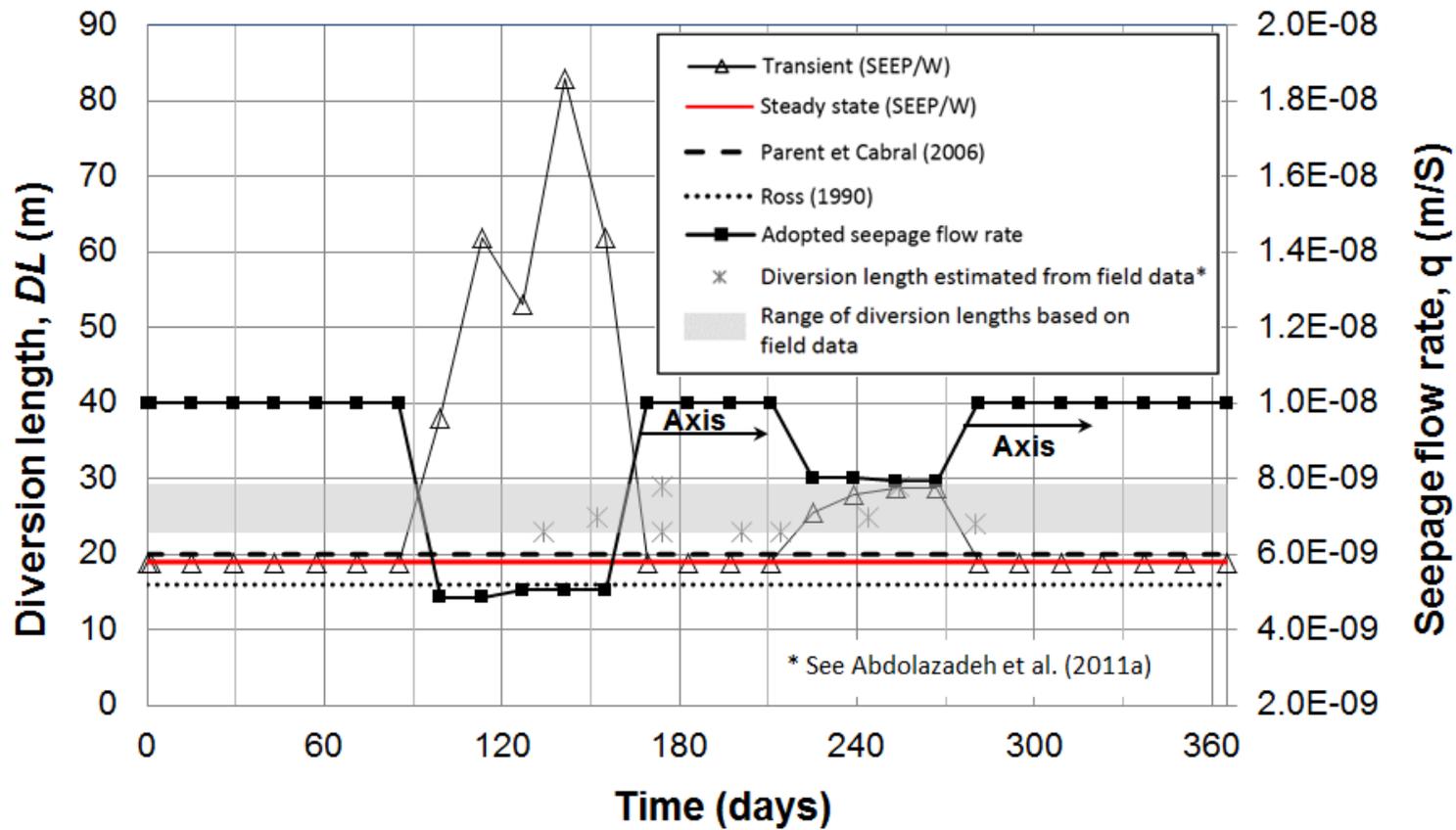Figure 4: Visual HELP modeling results of the seepage flow rates through the DBP layer during a typical year.

Figure 5: Evolution of the diversion length, as a function of the seepage flow rate (modified Visual HELP results, indicated as "adopted"; see Figure 4) and evolution of DL obtained by transient and, steady state analysis, as well as by using the Parent and Cabral (2006) and Ross (1990) models.